

# Thermodynamics of *n*-Alkane Mixtures and Polyethylene–*n*-Alkane Solutions: Comparison of Theory and Experiment

J. Luettmer-Strathmann,<sup>†</sup> J. A. Schoenhard, and J. E. G. Lipson\*

Department of Chemistry, Dartmouth College, Hanover, New Hampshire 03755

Received July 7, 1998; Revised Manuscript Received September 28, 1998

**ABSTRACT:** We have applied the lattice Born–Green–Yvon theory to the study of hydrocarbon mixtures. In doing so we have fit pure component data in order to determine characteristic parameters for the pure fluids and have used the geometric mean approximation for the mixed-segment interaction energy. As a result, we have been able to make predictions for a wide variety of solution properties without fitting any data on the mixtures and have compared our predictions with experimental results. For binary alkane solutions made from combinations of *n*-hexane, *n*-octane, *n*-decane, and *n*-hexadecane we have found excellent agreement between theory and experiment for pressure–volume isotherms, volume changes on mixing and its pressure dependence, and equilibrium solution vapor pressures as a function of composition and temperature. For polyethylene–*n*-alkane solutions we have been able to predict the lower critical solution temperature and its dependence on the chain length of the alkane solvent, as well as the full coexistence curve and its variation with the polymer molecular weight.

## Introduction

There has recently been considerable interest in studying mixtures of hydrocarbon fluids as a means of understanding more about polymer miscibility. Such studies are not new; indeed, they extend back over thirty years.<sup>1–14</sup> In our own work on developing the Born–Green–Yvon (BGY) integral equation method to describe fluids and their mixtures<sup>11,12,14</sup> the initial connections with experimental data focused on a series of hydrocarbon fluids,<sup>12</sup> which also gave us the opportunity to compare the BGY lattice model with existing theories.<sup>12,14</sup> In this paper we turn to hydrocarbon mixtures, for two main reasons: First, it seems prudent to initiate our work on mixtures by studying the simplest systems which are still of widespread interest. Hydrocarbons play an important role in polymer industry, yet they are relatively simple (at least structurally), and mixtures of hydrocarbons are capable of exhibiting interesting phase-separation behavior. For example mixtures of polyethylene and *n*-alkanes have a lower critical solution temperature (LCST) whose value depends on the chain length of the alkane solvent.<sup>2,4,7,8</sup> Turning to polymer mixtures, polyolefin blends are capable of the entire range of phase behavior, including both upper and lower critical solution temperatures, closed-loop phase diagrams, and so on.<sup>15</sup> Another reason for focusing on hydrocarbons is to exploit the wealth of data available for small-molecule mixtures as a means of checking the ability of the theory to predict a range of physical properties.

We begin by examining several *n*-alkane solutions, particularly the hexane–hexadecane mixture as that has been the most widely studied experimentally. Since we have had some success in using pressure–volume–temperature (*PVT*) data, we start by considering the *PVT* surface of the mixture<sup>16,17</sup> and then turn to other thermodynamic quantities of interest, such as the volume change on mixing<sup>18–22</sup> and the equilibrium vapor

pressure above the mixture.<sup>23,24</sup> For the polyethylene–*n*-alkane solutions we are primarily interested in the coexistence curve and its extremum, the LCST.<sup>2,4,7,8</sup> While it may not be realistic to expect quantitative agreement between experiment and theory over the entire range of experimental conditions, it is possible to test the ability of a theory to make predictions about trends.

In order to use our theoretical results to make predictions about fluid and mixture properties, we need values for the microscopic parameters which characterize these systems. For a pure (compressible) fluid there are three:  $\epsilon$ , the interaction energy acting between nonbonded segments;  $v$ , the volume per mole of lattice sites;  $r$ , the number of contiguous lattice sites needed to place a single molecule on the lattice. We are also interested in binary (compressible) mixtures. In this case we fix the volume per mole of lattice sites to the same value for each of the pure components and the mixture, which means that each of the pure components and the mixture are fitting into the same lattice. This will ensure that the “hard-core volume” of each component is independent of composition without having to resort to such artificialities as changing the effective number of segments for each composition studied. Note that this does *not* imply that the molar volumes of the pure components and the mixture are the same. Thus, in studying mixtures we first fit the pure fluid data in order to determine  $\epsilon_u$  and  $r_i$  with  $v$  fixed. The remaining parameter, and the one which characterizes the binary mixture, is the mixed interaction energy,  $\epsilon_{ij}$ . In this, our first study, we decided to follow the simplest possible approach by using the geometric mean approximation, that is

$$\epsilon_{ij} = (\epsilon_{ii}\epsilon_{jj})^{1/2} \quad (1)$$

For our studies on small hydrocarbon mixtures we use *PVT* data, as we also do for the polymeric fluids, and fit the BGY equation of state to the experimental *PVT* surface. However, in considering mixtures of *n*-alkanes with polyethylene, we realized that it would be advisable

<sup>†</sup> Present address: Department of Physics, The University of Akron, Akron OH 44325.

\* To whom correspondence should be addressed.

to fit data on the hydrocarbon solvent which spanned the same pressure–temperature range as that of the polymer solution. Thus, we turned to the liquid–vapor coexistence curve in order to find the  $n$ -alkane parameters for these mixtures. In the two subsequent sections we turn to a comparison of the theoretical predictions with experimental results on the mixtures: first, mixtures of small  $n$ -alkanes and, second, solutions of polyethylene in  $n$ -alkanes. In the last section we summarize our conclusions.

### Characterization of Pure Fluids and Mixtures

In previous work we showed that the BGY equation of state was very effective at describing the  $PVT$  surface for both small molecules and polymers.<sup>11,12,14</sup> Consider a lattice of coordination number  $z$ , partially occupied by molecules of type 1 and type 2; the rest of the lattice sites are vacant. Suppose that there are  $N_i$  chains of type  $i$ , each of which occupies  $r_i$  contiguous sites; the number of vacant sites, or holes, is denoted by  $N_h$ . The concentrations of the two components are denoted by site fractions,  $\phi_i$ , where

$$\phi_i = r_i N_i / N_{\text{total}} \quad \text{where} \quad N_{\text{total}} = N_h + \sum_i r_i N_i \quad (2)$$

We also define a concentration variable which accounts for the nearest-neighbor connectivity characteristic of chain molecules:

$$\xi_i = q_i N_i / N_q \quad \text{where} \quad N_q = N_h + \sum_i q_i N_i \quad (3)$$

with  $q_i z = r_i z - 2r_i + 2$ . Whereas  $r_i z$  gives the maximum number of nonbonded nearest-neighbor interactions possible for  $r_i$  unconnected segments,  $q_i z$  gives the maximum number possible when the  $r_i$  segments have been connected into a chain.

Derivations of the expression for the equation of state for a compressible fluid or mixture have been published elsewhere;<sup>25</sup> thus, we show here only the final result for a binary compressible mixture:

$$P = -(\beta v)^{-1} \left[ \ln \phi_h + \frac{z}{2} \ln \left( \frac{\xi_h}{\phi_h} \right) + \frac{z}{2} \left\{ \xi_1 \frac{\xi_1 [\exp(-\beta \epsilon_{11}) - 1] + \xi_2 [\exp(-\beta \epsilon_{12}) - 1]}{\xi_1 \exp(-\beta \epsilon_{11}) + \xi_2 \exp(-\beta \epsilon_{12}) + \xi_h} + \xi_2 \frac{\xi_1 [\exp(-\beta \epsilon_{12}) - 1] + \xi_2 [\exp(-\beta \epsilon_{22}) - 1]}{\xi_1 \exp(-\beta \epsilon_{12}) + \xi_2 \exp(-\beta \epsilon_{22}) + \xi_h} \right\} \right] \quad (4)$$

For all of this work the value of  $z$  was fixed at 6. The quality of the  $PVT$  fits did not depend on  $z$ , although the exact values of the parameters did change. As noted above, in all of the work involving mixtures  $v$  is fixed. In our work on hydrocarbon mixtures we first focused on the  $n$ -C6/ $n$ -C16 combination, in part because there are plentiful data available from a variety of sources for this mixture and in part because these two alkanes represented the boundaries in terms of chain length. To obtain the parameters  $\epsilon_{ij}$ ,  $r_{ij}$ , and the single value of  $v$ , the following data were fit simultaneously: ( $P$ ,  $T$ ,  $\rho$ ) sets (where  $\rho$  is density),<sup>16,17</sup> saturation vapor pressures, and coexistence liquid densities for both components, as well as coexistence vapor densities for  $n$ -C6 and the enthalpy of vaporization for  $n$ -C16.<sup>26</sup> For the other small alkanes studied the value of  $v$  was fixed at the value of 9.8577

**Table 1. Characteristic Parameters of  $n$ -Alkanes for Binary Alkane Mixtures**

alkane	$v$ (mL/mol)	$r$	$\epsilon$ (J/mol)
hexane	9.8577	11.130	−1503.5
octane	9.8577	14.143	−1565.6
dodecane	9.8577	20.192	−1639.8
hexadecane	9.8577	26.290	−1691.9

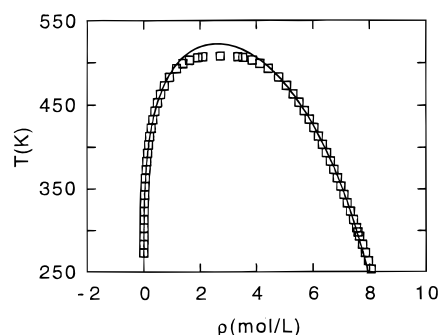


**Figure 1.** Liquid–vapor coexisting densities for  $n$ -hexane. The curve is the BGY fit to experimental data,<sup>26</sup> given by the symbols.

mL/mol which was determined in this fit, and similar data sets for each of the pure components<sup>17,26</sup> were fit to yield values of  $\epsilon_{ij}$  and  $r_{ij}$ . The collection of characteristic parameters obtained as described are tabulated in Table 1. In earlier work we showed that by fitting the liquid  $PVT$  surface for a series of  $n$ -alkanes the resulting parameters (including values of  $v$ , which was not fixed in that study) showed sensible variations with chain length.<sup>12</sup> We also noted how closely the hard-core volume,  $rv$ , tracked the van der Waals  $b$ -parameter, and illustrated how the maximum intermolecular interaction energy per molecule, directly proportional to  $\epsilon$ , increased with chain length for a series of homologous  $n$ -alkanes. Subsequent predictions for vapor pressures and critical points of these alkanes were in excellent agreement with experimental results. The same conclusions can be drawn for the parameters characterizing the components in this study, and the quality of the fits to the alkane  $PVT$  surface are equivalent to those shown in Figure 1 of ref 12.

Equation 4 was similarly fit to the  $PVT$  surface of polyethylene employing three different molar masses. The experimental data were in the molten region, with temperatures between 420 and 560 K and pressures between 10 and 200 MPa.<sup>15,27,28</sup> The results for the characteristic parameters are given in Table 2 and show that  $\epsilon$  and  $v$  are independent of the molar mass, while  $r$  is proportional to it. Over the temperature range of experimental interest the polymer densities predicted by the BGY theory differed from the experimental values typically by no more than 0.3%, increasing at most to 1% for the lowest pressures.<sup>29</sup>

In studying the  $n$ -alkane/polyethylene solutions it was important to obtain characteristic parameters for the  $n$ -alkanes which reflected the temperature and pressure range of the polymer solutions. Furthermore, since the effect of the chain length of the solvent was to be studied, consistent data sets for the different alkanes were required so that the influence of the chain length on the system-dependent parameters would not be masked by the distribution (in pressure and temperature) of the available experimental data sets. Finally, it is well-known<sup>2,7</sup> that the lower critical solution temperatures of the polymer solutions are close to the

**Table 2. Characteristic Parameters and Predicted LCST Values for PE-Alkanes**

alkane	$v$ (mL/mol)	$r$	$\epsilon$ (J/mol)	LCST (K) predicted
pentane	9.994499	9.505299	-1462.353	260.4
hexane	10.72353	10.35107	-1550.565	371.2
heptane	11.31877	11.22030	-1622.060	435.9
octane	11.81632	12.10191	-1681.552	484.0
nonane	12.24009	12.99011	-1732.088	522.8
decane	12.60660	13.88162	-1775.729	555.5
undecane	12.92766	14.77453	-1813.933	583.7
dodecane	13.21193	15.66765	-1847.756	608.6
tridecane	13.46595	16.56028	-1877.987	630.8
polyethylene <sup>a</sup>	9.621464	15890.72	-1988.320	
polyethylene <sup>b</sup>	9.621394	9629.90	-1988.458	
polyethylene <sup>c</sup>	9.623040	5663.81	-1988.729	

<sup>a</sup> Molar mass used for this polyethylene sample: 140 262 g/mol.

<sup>b</sup> Molar mass used for this polyethylene sample: 85 000 g/mol.

<sup>c</sup> Molar mass used for this polyethylene sample: 50 000 g/mol.

critical temperatures of the solvents. We therefore turned to liquid-vapor coexistence data. The coexisting densities ( $\rho_{\text{vap}}$ ,  $\rho_{\text{liq}}$ ) are determined through the following criteria

$$P(T, \rho_{\text{vap}}) = P(T, \rho_{\text{liq}}) \quad \mu(T, \rho_{\text{vap}}) = \mu(T, \rho_{\text{liq}}) \quad (5)$$

where  $\mu$  is the chemical potential. The data used for each alkane were restricted to within  $0.5T_c$  to  $0.9T_c$  (where  $T_c$  is the critical temperature) in order to ensure consistency between the different alkanes and to avoid the critical region. The alkane parameters are expected to be different from those in Table 1 because of the different temperature-pressure ranges of the data employed and because we are no longer insisting that  $v$  is fixed at 9.8577 mL/mol. Since vapor density data are not readily available for the higher *n*-alkanes, we decided to employ experimental coexistence density data of the lower alkanes to develop a correlation of the system-dependent parameters  $\epsilon$ ,  $r$ , and  $v$  as a function of  $n$  which could be extrapolated to the higher *n*-alkanes of interest. Hence, we determined  $\epsilon$ ,  $r$ , and  $v$  from a comparison of tabulated liquid and vapor densities<sup>26</sup> for the *n*-alkanes from methane to octane (with the exception of butane for which vapor densities were not listed). In the correlation of the parameters with chain length it became obvious that methane and ethane did not fit in well with the rest of the alkanes, so they were not included. The system-dependent parameters of the remaining alkanes were correlated with the aid of the following relationships:

$$\begin{aligned} rv &= 0.016n + 0.015 \\ r\epsilon &= -2150n - 3150 \\ (r)^{1/2} &= -0.877539 + 1.512447(n + 1.4651)^{1/2} \times \\ &\quad (n^{-1/2} + 0.58259) \end{aligned} \quad (6)$$

which reflect a special emphasis on the results for hexane through octane. The first two relationships illustrate the linear dependence of the hard-core volume ( $rv$ ) and interaction energy per mole ( $r\epsilon$ ), respectively, on chain length ( $n$ ); neither is expected to hold for very small  $n$ . The third relationship is the result of three observations: (a) Experimental values for the critical temperatures of the *n*-alkanes from  $n = 4$  to  $n = 24$ <sup>30</sup> are represented well by the correlation  $(T_c^{\text{exp}})^{1/2} = 0.0448n^{-1/2} + 0.0261$ . (b) The BGY lattice model yields the following relationship between the calculated criti-

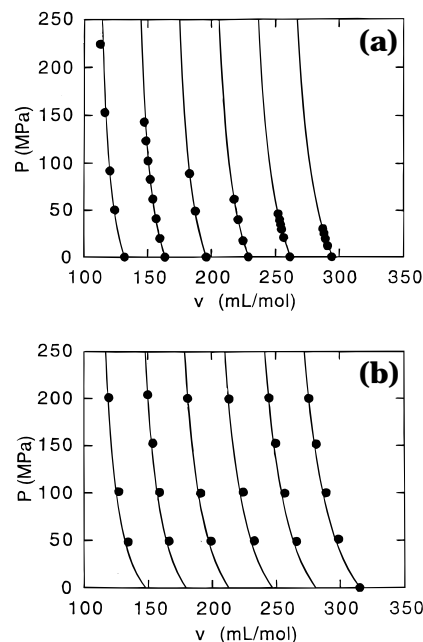


**Figure 2.** Pressure-volume data for mixtures of *n*-C6/*n*-C16. Each curve is an isopleth, with compositions ranging from (left to right) pure hexane to pure hexadecane in increments of 0.2 mole fraction of hexane. The symbols show experimental results;<sup>16</sup> the curves are the BGY predictions. Part (a) is for 298.15 K; part (b) is for 373.15 K.

cal temperature,  $T_c^{\text{BGY}}$ , and the parameters  $\epsilon$  and  $r$ :  $(T_c^{\text{BGY}}/|\epsilon|)^{-1/2} = 1.3534r^{-1/2} + 1.1872$ . (c) The critical temperatures predicted from the parameters of the alkane fits are on average 3% higher than the corresponding experimental values, so that  $T_c^{\text{exp}} \approx 0.971 T_c^{\text{BGY}}$ .

These correlations allow us to infer the parameter values for pentane through tridecane. The alkane parameters obtained in this way are summarized in Table 2, and a typical result is illustrated in Figure 1, which shows the BGY fit to the experimental liquid-vapor coexistence curve. Over the temperature range indicated above the predicted coexistence densities differed from the experimental values by about 5% or less, even for those alkanes whose characteristic parameters were extrapolated using eq 6, such as tridecane.

### Mixtures of *n*-Alkanes

In the previous section results were presented demonstrating the ability of the BGY equation of state to fit experimental data on pure fluids. Although we could apply eq 4 to fit the *PVT* surface of a mixture, we choose instead to use the pure component results for  $\epsilon_{ij}$  and  $r_i$  values from Table 1 in conjunction with eq 1 for the magnitude of  $\epsilon_{12}$  (the sign being negative) in order to predict the *PVT* surface for several alkane mixtures. For example, in Figure 2 we compare the BGY prediction for the *PVT* surface of the hexane-hexadecane mixture to the experimental results at two temperatures spanning the range of the experimental data.<sup>16</sup> Each of the curves is an isopleth, with compositions ranging from pure hexane to mixtures with hexadecane to pure hexadecane. The theory is able to do a very good job of predicting the *PVT* surface over the entire range of composition and temperature. Data sets on other hydrocarbon combinations are not as complete; typically



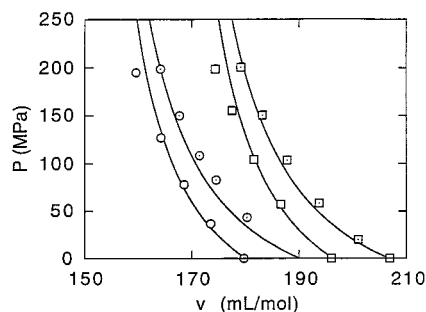


**Figure 3.** Pressure–volume isopleths for *n*-C6/*n*-C12 (circles) and *n*-C8/*n*-C12 (squares). The symbols represent experimental results<sup>17</sup> for two temperatures (298.15 K for the empty symbols and 348.15 K for the dotted symbols) and the curves are the BGY predictions.

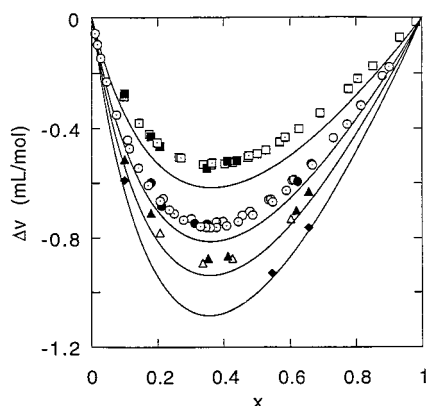


**Figure 4.** Volume change on mixing as a function of composition for *n*-C6/*n*-C16 at a series of temperatures. The solid lines are the BGY predictions for temperatures (from top to bottom) 293.15, 313.15, 323.15, and 333.15 K. The symbols are the corresponding experimental results from a variety of studies: filled symbols, ref 22; open circles and squares, ref 19; open triangles, ref 20; dotted circles, ref 18; dotted squares, ref 21.

only the equimolar mixture has been studied. Using the approach described above, we have found that the BGY predictions for such mixtures as *n*-C6/*n*-C12 and *n*-C8/*n*-C12 show similarly close agreement with experimental results.<sup>17</sup>

In Figure 3 two isotherms are given for each of these two solutions. At first glance the agreement between the BGY predictions and the experimental data does not appear to be as close as for the *n*-C6/*n*-C16 results; however, note that the scale on the abscissa is much expanded in the former case relative to the latter.

Continuing with our analysis of mechanical properties, we can also compare the BGY predictions with experimental data for the volume change on mixing. This is illustrated in Figure 4 which shows results for  $\Delta V_{\text{mix}}$  over the entire composition range with  $P = 0.1$  MPa and the temperature ranging from 293 to 323 K.<sup>18–22</sup> Recall that the BGY predictions are calculated using pure component data alone, making use of eq 1 for the mixed interaction energy. Note that the values for  $\Delta V_{\text{mix}}$  are very small, being on the order of  $10^{-4}$  L mol<sup>-1</sup>, while the molar volumes of the mixtures are on the order of  $10^{-1}$  L mol<sup>-1</sup>. The theoretical curves are the right sign and shape and agree reasonably well with the experimental results at lower temperatures and very well at higher temperatures.<sup>31</sup> Although we do not have error bars on the experimental points, data from a number of labs are shown and this gives a sense of the precision. In Figure 5 data are plotted for the

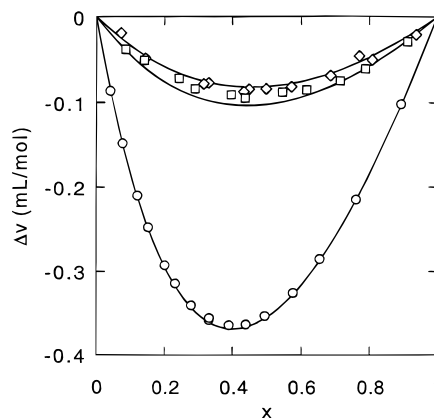


**Figure 5.** Volume change on mixing as a function of composition (mole fraction of lowest alkane) at 298.15 K and atmospheric pressure for *n*-C6/*n*-C8 (diamonds<sup>33a</sup>), *n*-C8/*n*-C12 (squares<sup>33b</sup>), and *n*-C6/*n*-C12 (circles<sup>32</sup>). The curves are the BGY predictions.

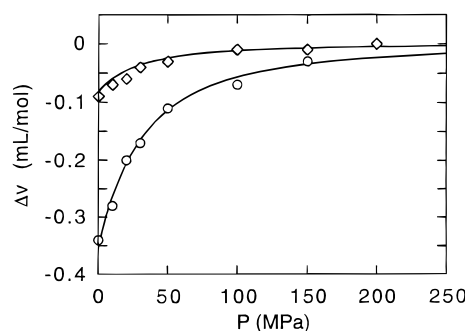


**Figure 6.** Comparison between experimental results<sup>34</sup> and BGY predictions for the volume change on mixing as a function of pressure for a 0.5 mole fraction mixture of *n*-C6/*n*-C8 (diamonds) and *n*-C6/*n*-C12 (circles) at 298.15 K.

volume change on mixing of three additional mixtures, *n*-C6/*n*-C12,<sup>32</sup> *n*-C6/*n*-C8, and *n*-C8/*n*-C12,<sup>33</sup> all at 293 K. Once again, the theory is doing well at predicting these very small volume changes on mixing. In addition to temperature and composition, pressure is another experimental variable which may be controlled. Figure 6 illustrates the pressure variation of the volume change on mixing for two mixtures, *n*-C6/*n*-C8 and *n*-C6/*n*-C12, at 293 K.<sup>34</sup> The BGY predictions for the effect of changing pressure from atmospheric (0.1 MPa) up to 200 mPa agree very closely with experimental results for both mixtures.

In the section which follows we shall make predictions on the miscibility of hydrocarbon solutions which phase separate. While the small alkane mixtures discussed here show no such behavior, we can still test theory against experiment for the free energy of the mixture, as reflected in the total vapor pressure above the solution at equilibrium and how this changes with composition and temperature. In Figure 7 we show the saturation pressure above an *n*-C6/*n*-C16 solution as a function of mole fraction of hexane for a series of temperatures ranging from 293 to 333 K. The data symbols represent results from different experimental groups,<sup>23,24</sup> while the solid lines are the BGY predictions. Recall that Raoult's law (for any given temperature) would predict a straight line connecting two points: the pure hexane vapor pressure at mole fraction of hexane equal to 1, and the pure hexadecane vapor pressure at mole fraction of hexane equal to zero. Since the pure vapor pressure of hexadecane is very small

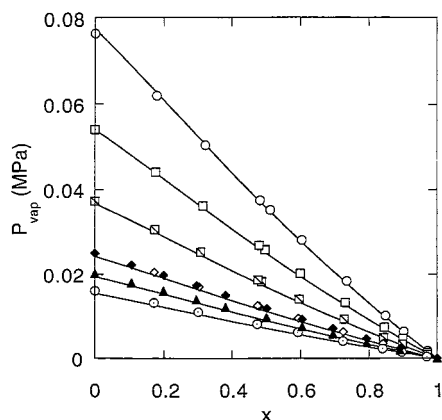


**Figure 7.** Temperature dependence of the vapor pressure of *n*-C6/*n*-C16 as a function of composition for a series of temperatures (from top to bottom: 333.15, 323.15, 313.15, 303.15, 298.15, and 293.15 K). The symbols represent experimental results (filled symbols, ref 23; open symbols, ref 24) and the lines are the BGY predictions.

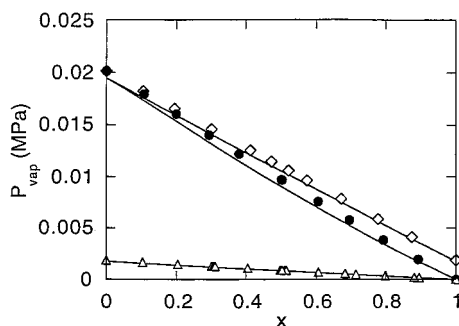


**Figure 8.** Comparison between experiment<sup>23</sup> and BGY predictions for vapor pressure as a function of composition (mole fraction of highest alkane) for *n*-C6/*n*-C8 (diamonds), *n*-C6/*n*-C16 (circles), and *n*-C8/*n*-C16 (triangles) at 298.15 K. The curve for *n*-C8/*n*-C16 is an extrapolation for *x*(*n*-C16) above 0.5.

compared to that of hexane (numbers here at 298 K), the latter appears as zero on the plot. The BGY predictions agree very closely with the experimental results, even reproducing the minor deviations from Raoult's law behavior, which become more obvious at higher temperatures. In Figure 8 the results at 293 K for *n*-C6/*n*-C16 are shown in comparison to results for *n*-C6/*n*-C8 and *n*-C8/*n*-C16.<sup>23</sup> On this expanded scale (relative to that of Figure 7) small differences can be seen between the BGY predictions for *n*-C6/*n*-C16 and the experimental data; agreement between theory and experiment is even closer for the other two mixtures. Note that the vapor pressure of pure *n*-C8 is considerably lower than that of *n*-C6, resulting in very small values for the equilibrium vapor pressures above the *n*-C8/*n*-C16 solution. Even so, the BGY prediction, which is shown for mole fraction of octane up to 0.5, is still in excellent agreement with experiment. For larger concentrations of octane the line has been extrapolated since solving for the tiny vapor pressure values proved to be somewhat tedious. Although the temperature dependence of the vapor pressure above an alkane mixture has not been extensively studied for mixtures other than *n*-C6/*n*-C16 we did find results at two temperatures for the mixture *n*-C6/*n*-C8, illustrated in Figure 9.<sup>23,35</sup> These results, for 293 and 323 K, confirm that the combination of the BGY theory with the geometric mean approximation yields very close agreement with experimental results on mixtures, making

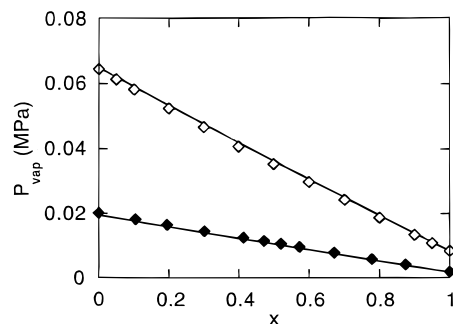


**Figure 9.** Temperature dependence of the vapor pressure as a function of composition for *n*-C6/*n*-C8. Symbols are experimental results (open, 328.15 K;<sup>35</sup> filled, 298.15 K<sup>23</sup>) and lines are BGY predictions.

use of pure component data alone.

### Phase Separation in Solutions of Polyethylene with *n*-Alkanes

The logical next step in the progression to the study of hydrocarbon polymer mixtures is to study polymer solutions, hence the choice of polyethylene (PE) dissolved in different *n*-alkanes. It is well-documented that such solutions show LCSTs at ambient pressure, with the value of the critical temperature increasing as the chain length of the alkane increases;<sup>2,4,7,8</sup> our goal was to capture this behavior using the approach described above. The characteristic parameters for the *n*-alkanes and those for the polymer samples are listed in Table 2. For the studies on alkane mixtures, fixing the value of  $v$  ensured that both components fit onto the same lattice and that the volume change on mixing approached zero in the limit of pure component 1 or 2. In this case we achieve the same result for each mixture by choosing  $v$  to be the alkane (component 1) value and then renormalizing  $r$  for the polymer (component 2) such that the product  $r_2 v_2$  (the hard-core volume of a polymer molecule on the lattice) remains constant. In other words, for the polymer we take  $r_2(\text{new}) = r_2(\text{old}) v_2 / v_1$ . As described above, we use eq 1 for the remaining parameter,  $\epsilon_{12}$ .

The critical point for our binary mixture is defined by the following equations:<sup>36</sup>

$$\left(\frac{\partial \mu}{\partial x}\right)_{T,P} = \left(\frac{\partial \mu}{\partial x}\right)_{T,\rho} - \rho^2 \left(\frac{\partial \mu}{\partial \rho}\right)_{T,x} \left(\frac{\partial \rho}{\partial x}\right)_{T,x} = 0$$

$$\left(\frac{\partial^2 \mu}{\partial x^2}\right)_{T,P} = 0 \quad (7)$$

where  $\rho$  is the total molar density, defined as  $\rho = \rho_1 + \rho_2$ ,  $x = \rho_2 / \rho$  is the mole fraction of polymer, and  $\mu = \mu_2 - \mu_1$  is the difference in chemical potential between the polymer and solvent. The first of the two equations defines the spinodal curve and the second identifies the critical point as the extremum of the spinodal.  $\rho$  and  $x$  can be related to the site fractions of the two components through

$$\rho = \frac{1}{v} \left( \frac{\phi_1}{r_1} + \frac{\phi_2}{r_2} \right), \quad x^{-1} = 1 + \frac{\phi_1 r_2}{r_1 \phi_2} \quad (8)$$

In order to determine the critical temperature for the polyethylene-alkane mixtures, eq 7 was solved numerically at atmospheric pressure ( $P = 0.1$  MPa). For each case a plot of the spinodal as a function of  $x$  yields the

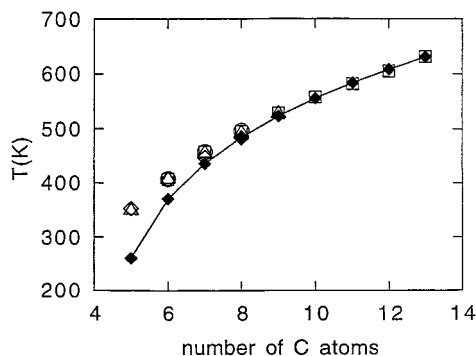


**Figure 10.** Comparison of the *predicted* lower critical solution temperatures with experimental results<sup>2,4,7,8</sup> for polyethylene in a series of *n*-alkanes, plotted as a function of the number of carbons in the alkane chain.

LCST as the minimum of the curve. A comparison of the BGY predictions with experimental results<sup>2,4,7,8</sup> for the polyethylene–alkane LCST as a function of the alkane chain length is shown in Figure 10 and the results are summarized in Table 2. For the higher alkanes, down to about *n*-heptane, the agreement between theory and experiment is very close, demonstrating that the combination of the BGY theory with the geometric mean approximation continues to do well with these straight-chain hydrocarbon mixtures, even as the disparity between the chain length of the components becomes large. For the shorter alkane solvents the agreement is not quite as good. This may indicate the limitations of eq 1 in the sense that the effectiveness of the geometric mean approximation is expected to deteriorate as the solvent and solute become increasingly dissimilar. Although both components are still hydrocarbons, the difference in chain length may be enough to temper the effectiveness of assuming that each molecule experiences an averaged environment, especially in the polymer–solvent case where the critical composition is relatively dilute in polymer.

The full coexistence curve, or binodal, can be mapped out using the criteria that the chemical potential is the same in coexisting phases (say I and II) for each of the components; that is,

$$\mu_1(T, P, x_I) = \mu_1(T, P, x_{II}), \quad \mu_2(T, P, x_I) = \mu_2(T, P, x_{II}) \quad (9)$$

The results for three different molar mass samples of polyethylene in *n*-decane are shown in Figure 11. The ordinate is the temperature relative to the LCST where the experimental LCST was used in plotting the data points<sup>7</sup> and the BGY prediction for the LCST was used in plotting the curves. As Table 2 indicates, the difference between the experimental and predicted LCST value was but a tiny percentage of the critical temperature. The abscissa is the concentration in mass fraction

$$c = M_2 x / [M_2 x + M_1 (1 - x)] \quad (10)$$

which we use here because the mole fractions of the solutions are such small numbers. The results show that both the shape of the coexistence curve and the effects of varying the molar mass are captured by the BGY theory without having to fit any data on the mixtures themselves.

## Discussion

The results presented here represent our first efforts in using the BGY theory of lattice mixtures to describe

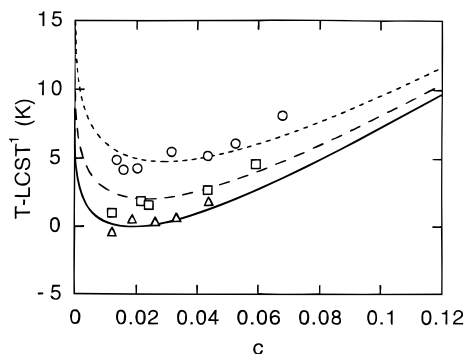


**Figure 11.** Coexistence curves for polyethylene in *n*-C10 as a function of the mass fraction polymer, at 0.1 MPa. From top to bottom the molar mass of polyethylene used was (in g/mol): 50 000, 85 000 and 140, 262. In plotting these curves the LCST of the highest molar mass sample has been subtracted from both the experimental<sup>5</sup> (LCST of 557.6 K) and theoretical (LCST of 555.7 K) results.

solutions of experimental interest and build on our previous work on pure hydrocarbon fluids using the lattice BGY equation of state. These efforts in the realm of hydrocarbons were originally motivated by the perception that the range and quality of data were such that we could adequately test the BGY theory. Continuing with our incremental approach in applying the theory, we have chosen to stay with hydrocarbons and investigate mixtures whose components are very similar, differing only in their chain length. As clear from experimental results, even this apparently small difference may lead to interesting miscibility behavior.

The BGY theory has the same kind of microscopic parameters as those of other theories of its type.<sup>1,3,5,6,9,10,13</sup> In describing mixtures most of the parameters characterize the pure components, and obtaining values for these by fitting experimental data is routine. The parameter (or parameters) characterizing the mixture represents more of a problem. A typical route to a value for this is also via fitting, but of data on the mixture.<sup>1,5,6,13</sup> For mixtures exhibiting limited miscibility one choice is to fit the extremum of the coexistence curve;<sup>5</sup> of course, this requires that such data are already available. If the goal of using such a theory is to make predictions about the miscibility of the mixture, then this approach does not seem extremely practical. More recently, small-angle neutron-scattering data have been used.<sup>13</sup> Different issues arise here, involving (among other things) the assumption of incompressibility. For mixtures which are completely miscible (for example, some of the alkane solutions) various data have been fit;<sup>5</sup> sometimes data for different temperatures have been used to obtain temperature-dependent values for  $\epsilon_{12}$ .<sup>37</sup> When mixture properties are used to determine the system-dependent parameters, including those of the mixture itself, equations of state typically describe mixture data very well.<sup>1,5,6,13</sup> We have chosen to postpone decisions involving the kind and amount of data needed to characterize a mixture by focusing on simple mixtures and using the geometric mean approximation. In doing so we are trying to ascertain just how far this approximation can be taken before it begins to break down. In the work presented here we have found that using eq 1 for the mixed interaction energy has led us to predictions about properties of hydrocarbon mixtures which are in good-to-excellent agreement with experimental results. For the simple alkane mixtures we were able to predict *PVT* curves which corresponded



extremely well with the experimental data. In addition, the very small volume changes on mixing for these solutions were also predicted by the BGY theory, as was the pressure dependence of this quantity. Further agreement with experimental results was shown in predictions of the solution free energy, as characterized by its equilibrium vapor pressure, as a function of composition and temperature. Turning to solutions of polyethylene with *n*-alkane solvents, the BGY theory is able to predict the chain-length dependence of the LCST with critical point values, especially for *n*-heptane and higher, which are in excellent agreement with experiment. Further, the BGY theory also yields accurate predictions for the complete coexistence curve and the effect on it of varying the molecular weight of the polymer. All of the BGY predictions on the mixture properties were made without using any mixture data for fitting purposes.

Recently, there has been considerable interest in hydrocarbon (polyolefin) polymer blends, motivated by a careful set of studies undertaken by Lohse, Graessley, and co-workers<sup>15</sup> who have shown that such blends are capable of exhibiting the full range of interesting phase behavior. The work described in this paper has put us in the position of being able to tackle the issue of miscibility in polyolefin blends. Such studies are now in progress and will allow us to determine the extent to which the BGY theory in conjunction with the geometric mean approximation may be pushed in the description of complex fluid mixtures.

**Acknowledgment.** Financial support from the National Science Foundation (DMR-9424086 and DMR-9730976) and the Camille and Henry Dreyfus Foundation has made this research possible. The authors are also grateful to D. J. Lohse for supplying data on polyethylene.

## References and Notes

- (1) Flory, P. J.; Orwoll, R. A.; Vrij, J. A. *J. Am. Chem. Soc.* **1964**, *86*, 3515.
- (2) Orwoll, R. A.; Flory, P. J. *J. Am. Chem. Soc.* **1967**, *89*, 6822.
- (3) Patterson, D.; Delmas, G. *Trans. Faraday Soc.* **1968**, *65*, 708.
- (4) Hamada, F.; Fujisawa, K.; Nakajima, A. *Polym. J.* **1973**, *4*, 316.
- (5) Lacombe, R. H.; Sanchez, I. C. *J. Chem. Phys.* **1976**, *80*, 2568.
- (6) Sanchez, I. C.; Lacombe, R. H. *Macromolecules* **1978**, *11*, 1145.
- (7) Kodama, Y.; Swinton, F. L. *Brit. Polym. J.* **1978**, *10*, 191.
- (8) Charles, G.; Delmas, G. *Polymer* **1981**, *22*, 1181.
- (9) Bawendi, M.; Freed, K. F. *J. Chem. Phys.* **1987**, *87*, 5535.
- (10) Curro, J. G.; Schweizer, K. S. *J. Chem. Phys.* **1987**, *87*, 1842.
- (11) Lipson, J. E. G. *J. Chem. Phys.* **1992**, *96*, 1418.
- (12) Lipson, J. E. G.; Andrews, S. S. *J. Chem. Phys.* **1992**, *96*, 1426.
- (13) Dudowicz, J.; Freed, K. F. *Macromolecules* **1995**, *28*, 6625.
- (14) Lipson, J. E. G. *Macromol. Theory Simul.* **1998**, *7*, 263.
- (15) Krishnamoorti, R.; Graessley, W. W.; Dee, G. T.; Walsh, D. J.; Fetters, L. J.; Lohse, D. J. *Macromolecules* **1996**, *29*, 367 and references cited therein.
- (16) Dymond, J. H.; Young, K. J.; Isdale, J. D. *J. Chem. Thermodyn.* **1979**, *11*, 887.
- (17) Dymond, J. H.; Robertson, J.; Isdale, J. D. *J. Chem. Thermodyn.* **1982**, *14*, 51.
- (18) Marsh, K. N.; Organ, P. P. *J. Chem. Thermodyn.* **1985**, *17*, 835.
- (19) Reeder, J.; Knobler, C. M.; Scott, R. L. *J. Chem. Thermodyn.* **1975**, *7*, 345.
- (20) Holleman, T. *Physica* **1963**, *29*, 585.
- (21) Desmyter, A.; Van der Waals, J. H. *Recueil* **1958**, *77*, 53.
- (22) Diaz Peña, M.; Benítez de Soto, M. *Ann. Fis. Quim.* **1965**, *61-B*, 1163.
- (23) Weiguo, S.; Qin, A. X.; McElroy, P. J.; Williamson, A. G. *J. Chem. Thermodyn.* **1990**, *22*, 905.
- (24) McGlashan, M. L.; Williamson, A. G. *Trans. Faraday Soc.* **1961**, *57*, 588.
- (25) Lipson, J. E. G.; Brazhnik, P. K. *J. Chem. Phys.* **1993**, *98*, 8178.
- (26) *Tables on the Thermophysical Properties of Liquids and Gases*, 2nd ed.; Vargaftik, N. B., Ed.; Hemisphere Publishing Corp.: Washington, D.C., 1975.
- (27) Walsh, D. J.; Graessley, W. W.; Datta, S.; Lohse, D. J.; Fetters, L. J. *Macromolecules* **1992**, *25*, 5236.
- (28) Tabulated PVT data for polyethylene were kindly sent to us by Dr. D. Lohse.
- (29) Luettmer-Strathmann, J.; Lipson, J. E. G. *Fluid Phase Equilib.* **1998**, *150–151*, 649.
- (30) Ambrose, D.; Tsonopoulos, C. *J. Chem. Eng. Data* **1995**, *40*, 531.
- (31) The results summarized here supercede those preliminary mixing results reported in ref 1, which were compromised by a small mistake in the calculation of the equilibrium densities.
- (32) Hamam, S. E. M.; Kumaran, M. K.; Benson, G. C. *J. Chem. Thermodyn.* **1984**, *16*, 537.
- (33) (a) Goates, J. R.; Ott, J. B.; Grigg, R. B. *J. Chem. Thermodyn.* **1981**, *13*, 907. (b) Grigg, R. B.; Goates, J. R.; Ott, J. B. *J. Chem. Thermodyn.* **1982**, *14*, 101.
- (34) Katzenski, G.; Schneider, G. M. *J. Chem. Thermodyn.* **1982**, *14*, 801.
- (35) Gmehling, J.; Onken, U.; Kolbe, B. In *Vapor-Liquid Equilibrium Data Collection*; Behrens, D.; Eckermann, R., Eds.; DECHEMA: Frankfurt/Main, 1977; Vol. 1, Part 6c.
- (36) Rowlinson, J. S.; Swinton, F. L. *Liquids and Liquid Mixtures*, 3rd ed.; Butterworths: London, 1982.
- (37) Guggenheim, E. A. *Discuss. Faraday Soc.* **1953**, *15*, 24.

MA981063T